Electro oxidation of Malachite Green and Modeling Using ANN

P. Antony Soloman,[a] C. Ahmed Basha,[b,*] M. Velan,[a] and N. Balasubramanian[a]
[a]Department of Chemical Engineering, A. C. Tech Campus, Anna University-Chennai, Chennai-600 025, India
[b]Central Electrochemical Research Institute, Karaikudi-630 006, Tamilnadu, India

Original scientific paper
Received: April 12, 2010
Accepted: October 26, 2010

This study involves the electro-oxidation of malachite green, a triphenyl methane dye, extensively used in industries and aquaculture, and later banned in most developed countries because of its potential carcinogenicity, mutagenicity and teratogenicity in mammals. The study is conducted in a batch electro-chemical reactor using the catalytic anode (made of noble oxide coated, RuO_x-TiO_x, titanium expanded mesh) that mediates the oxidation of organic species by the formation of higher oxidation state oxides of the metal (e.g., RuO_2 or IrO_2). The operating variables are current density, electrolysis time and initial dye concentration. Complete removal of the dye has been reported by 41 minutes of treatment at a current density of 2.2 A dm^{-2} for the case of initial dye concentration of 200 mg L^{-1}. The experimental data are modeled using back-propagation artificial neural network. The results were compared with experimental observations, and found that the model predictions adequately match experimental observations. Combination of the factors giving complete removal of the dye has also been commented.

Key words:
Electro-oxidation, malachite green, artificial neural network, modeling

Introduction

Malachite green (MG) is a synthetic dye, used extensively in industries to color silk, wool, jute, leather, ceramics, cotton and paper. It has also been used as a bactericide, fungicide and parasiticide in aquaculture industries worldwide. It was one of the most widely used dyes in the family of triphenyl methane. The presence of MG in a water body can significantly affect the photosynthetic activity in aquatic life because of reduced light penetration and may also be toxic to some aquatic life by causing detrimental effects in liver, gill, kidney, intestine and gonads. In humans, it may cause irritation to the gastrointestinal tract upon ingestion. Contact of MG with skin causes irritation, redness and pain. Contact with eye will lead to permanent injury.[1] Being a member of the triphenylmethane family, MG is a suspected animal carcinogen. The potential carcinogenic, genotoxic, mutagenic and teratogenic properties of MG have been reported in many animal species and cell lines.[2]

MG and its reduced form, leuco MG, may persist in edible fish tissues for extended periods of time. Therefore, there are both environmental and human health concerns about bioaccumulation of MG and leuco MG in terrestrial and aquatic ecosystems. Even though MG is effective in both the applications as pointed out, its use has been banned in most developed countries, due to the health and environmental issues. Therefore, an effective technique is necessary for the treatment of wastewater containing MG.

Removal of color from dye-bearing wastewater is a complex problem because of the difficulty in treating such wastewaters by conventional methods. The effluent is characterized by high chemical oxygen demand (COD), total organic carbon, salt content and strong color. Aerobic degradation of triphenylmethane dyes has been demonstrated repeatedly; however, these dyes resist degradation in activated sludge systems. The chemical precipitation method generates considerable quantity of sludge and demands further treatment. On the other hand, the activated carbon adsorption has the associated cost and difficulty of regeneration. In recent years, there has been special focus on adopting advanced oxidation techniques such as electrochemical oxidation, photochemical oxidation, ozonation etc. In the electrochemical technique, the main reagent is electron; a 'clean reagent'. The technique offers high removal rate, high conversion; and consumes less energy in comparison with the non-electrochemical counterparts.[3] In recent years, there has been increasing interest in the use of electrochemical techniques for the treatment of various synthetic dyes.[4,5]

*Corresponding author: Tel +91 4565 227550; Fax: +91 4565 227713; Mobile: 9994221103; cab_50@rediffmail.com, basha@cecri.res.in (C. Ahmed Basha)

Korbahti *et al.*[6] has studied the electrochemical treatment of simulated textile wastewater containing Levafix Blue CA reactive dye in a batch cell and reported more than 90 % COD removal. Muthukumar *et al.*[7] studied the electro coagulation of CI Acid orange 10 from aqueous solutions in a batch cell and reported 60 % dye removal. An elegant indirect electrochemical study by electro-Fenton method on MG mineralization has been reported for oxidation pathways of malachite green by Fe^{3+}-catalized electro-Fenton process.[8] Mechanism of electro-oxidation of various dyes has been studied in pollutant centered approach by many researchers.[4,9] Such a study has not been elucidated for MG. The present study focuses on the modeling of electro-oxidation of MG dye by artificial neural network (ANN).

One of the characteristics of modeling based on ANN is that it does not require the mathematical description of the phenomena involved in the process and the fundamental element of ANN is the processing elements called neurons. ANN learns the latent relationships between the inputs and outputs without prior knowledge about the functional relationship between them. The elasticity of ANN enables updating the network with new data. The processing style of neural network is parallel and there is no strict rule or algorithm to follow. Further, ANNs are known as universal function approximators and they try to provide a tool that both programs learn on their own. Provision of model free solutions, data error tolerance, built in dynamism and lack of any exogenous input requirement makes ANN attractive.[10,11]

Mechanism of electro oxidation

The mechanism of electrochemical oxidation of wastewater is a complex phenomenon involving coupling of electron transfer reaction with a dissociate chemisorption step. Basically two different processes occur at the anode; on anode having high electro-catalytic activity, oxidation occurs at the electrode surface (direct electrolysis); on metal oxide electrode, oxidation occurs via surface mediator on the anodic surface,[12–14] where they are generated continuously (indirect electrolysis). The electrochemical oxidation of organic contaminants on noble oxide coated catalytic anode (RuO_x-TiO_x) is as follows.

In the first step, H_2O is discharged at the anode to produce adsorbed hydroxyl radicals according to the reaction.

$$RuO_x\text{-}TiO_x + H_2O \rightarrow RuO_x\text{-}TiO_x\,(^{\bullet}OH) + H^+ + e^- \quad (1)$$

In the second step, generally the adsorbed hydroxyl radicals may interact with the oxygen already present in the oxide anode with possible transition of oxygen from the adsorbed hydroxyl radical to the oxide forming the higher oxide RuO_x-TiO_{x+1}.

$$RuO_x\text{-}TiO_x\,(^{\bullet}OH) \rightarrow RuO_x\text{-}TiO_{x+1} + H^+ + e^- \quad (2)$$

At the anode surface the active oxygen can be present in two states, either as physisorbed RuO_x-TiO_x ($^{\bullet}OH$) or/and as chemisorbed RuO_x-TiO_{x+1}. When NaCl is used as supporting electrolyte, chloride ion may anodically react with RuO_x-TiO_x ($^{\bullet}OH$) to form adsorbed OCl^- radicals according to the following:

$$RuO_x\text{-}TiO_x\,(^{\bullet}OH) + Cl^- \rightarrow RuO_x\text{-}TiO_x\,(^{\bullet}OCl) + H^+ + 2\,e^- \quad (3)$$

In the presence of chloride ion, the adsorbed hypochlorite radicals may interact with the oxygen already present in the oxide anode with possible transition of oxygen from the adsorbed hypochlorite radical to the oxide forming the higher oxide RuO_x-TiO_{x+1} according to the following reaction and also RuO_x-TiO_x($^{\bullet}OCl$) simultaneously react with chloride ion to generate active oxygen (dioxygen) and chlorine according to the following reactions:

$$RuO_x\text{-}TiO_x\,(^{\bullet}OCl) + Cl^- \rightarrow RuO_x\text{-}TiO_{x+1} + Cl_2 + e^- \quad (4)$$

$$RuO_x\text{-}TiO_x\,(^{\bullet}OCl) + Cl^- \rightarrow RuO_x\text{-}TiO_x + \frac{1}{2}O_2 + Cl_2 + e^- \quad (5)$$

The reactions of anodic oxidation of chloride ions to form chlorine in bulk of solution as given by eqs. (4) and (5) proceed as follows:

$$Cl_2 + H_2O \rightarrow H^+ + Cl^- + HOCl \quad (6)$$

$$HOCl \rightleftharpoons H^+ + OCl^- \quad (7)$$

$$Dye + OCl^- \rightarrow CO_2 + H_2O + Cl^- + P \quad (8)$$

where P represents the other byproducts such as N_2 and some lower stable acids (acetic acids, formic acids etc). Since organic compounds of the effluent are electrochemically inactive, the primary reaction that occurs at the anodes is chloride ion oxidation (eqs. (4) and (5)) with the liberation of Cl_2, which is a robust oxidizing agent. As regards the reactions in the bulk, gaseous Cl_2 dissolves in the aqueous solutions due to ionization as indicated in eq. (6). The following reaction takes place in the cathode:

$$2H_3O^+ + 2e^- \rightarrow H_2 + 2H_2O \qquad pH < 7 \quad (9)$$

$$2H_2O + 2e^- \rightarrow H_2 + 2OH^- \qquad pH > 7 \quad (10)$$

Here, the rate of oxidation depends on the electrode activity, pollutants diffusion and current density. Indirect electrolysis refers to the processes in which a dissolved redox reagent either exists in or is generated from the electrolyte or from the electrode phase in order to participate in the targeted reaction.[15] Temperature, pH and diffusion of generated oxidants determine the rate of oxidation in indirect electrolysis.

In indirect electro-oxidation chloride salts of sodium are added in the dye solution for better conductivity and generation of hypochlorite ions. The generated hypochlorite ions act as main oxidizing agent in the pollutant degradation. A generalized reaction scheme of electrochemical conversion/combustion of organic pollutants on noble oxide coated anode is available in the literature.[12–17] Eq. (8) proposes that the dye present in the effluent is converted into CO_2 with the help of generated hypochlorite ions.

Materials and methods

Experimental

The chemical structure of MG, also called aniline green, basic green 4, diamond green B, or victoria green B, IUPAC name: 4-[(4-dimethylaminophenyl)-phenyl-methyl]-N, N-dimethyl-aniline, is illustrated in Fig. 1.

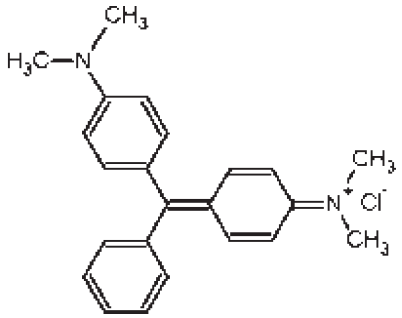

Fig. 1 – *Chemical structure of malachite green*

The MG sample was obtained from Qualigens Fine Chemicals, Mumbai, India. The chemicals used in the study were of analytical grade. The electrochemical oxidation of MG was studied in a batch electrochemical reactor using commercially available anode made of Ti/RuO_x-TiO_x coated expanded mesh,[18] and stainless steel as cathode respectively. A glass cylinder of 500 mL capacity was used as the batch electrochemical reactor. The electrodes were kept 2 cm apart. An electrode area (A) of 2.7 cm x 5.00 cm, accounting 13.5 cm^2 was exposed for the operation.

The synthetic MG dye effluent was prepared by dissolving the appropriate amount of dye in double distilled water. A sample volume of 300 mL, adjusted to a pH of 7 and electrolyte (NaCl) concentration of γ = 3 g L^{-1} was considered in every run. The reaction was started with the application of specified current density for the required initial dye concentration. A magnetic stirrer was used for homogenization. Experiments were carried out under constant current conditions using a DC-regulated power source (HIL model 3161) of 0–2 A and 0 – 30 V. The samples were allowed to settle for 30 min before analysis. Totally, 125 data were collected in random combination of factors within the experimental domain (current density, j = 0.4 – 2.2 A dm^{-2}; electrolysis time, t = 9 – 60 min; and initial dye concentration, γ_0 = 200 – 1200 mg L^{-1}) for the development of ANN model.

In order to determine the extent of effluent degradation, the COD was measured. The COD, as the name implies, is the oxygen requirement of a sample for oxidation of organic and inorganic matter. COD is generally considered as the oxygen equivalent of the amount of organic matter oxidizable by potassium dichromate. The organic matter of the sample is oxidized with a known excess of potassium dichromate in a 50 % sulfuric acid solution. The excess dichromate is titrated with a standard solution of ferrous ammonium sulfate solution. The CODs of all samples were determined by the dichromate open reflux method.

The UV/VIS spectrum of MG and its change during electro-oxidation was recorded using UV/VIS spectrophotometer (Elico SL 164 double beem UV/VIS spectrophotometer). The characteristic peak of pure MG was observed at λ = 617 nm. The dye concentrations in terms of COD values were calculated using a previously prepared calibration chart.

Artificial neural network

Most applications require networks that contain at least three normal types of layers-input, hidden, and output. The number of the layers and processing elements in the layers vary from one process to another. The user must determine the optimal number of layers and neurons. Generally, the number of layers and processing elements are defined by trial and error. The back-propagation method is a first-order gradient method of ANN. The training of a back-propagation neural network consists of two phases: a forward pass during which the processing of information occurs from the input layer to the output, and a backward pass when the error from the output layer is propagated back to the input layer and the interconnections are modified.[19]

In the present study, feed-forward ANN model is designed in back-propagation training algorithm using the neural network toolbox of MATLAB 7. The number of neurons in input and output layers depends on independent and dependent variables, respectively. Since one dependent variable- percentage removal of dye; depend on three variables- current density, electrolysis time and initial dye concentration; one and three neurons were devoted to output and input layers respectively. All inputs and outputs were normalized linearly before entering in ANN, using the following equation:[20]

$$A_i = \frac{(X_i - X_{\min})}{(X_{\max} - X_{\min})}(r_{\max} - r_{\min}) + r_{\min} \quad (11)$$

where X_i is input or output of the network, A_i is the normalized value of X_i, $X_{\min}$ and $X_{\max}$ are extreme values of X_i, and $r_{\min}$ and $r_{\max}$ define the limits of the range where X_i is scaled. In this work, input and output data are normalized between –1 and 1; and 0.2 and 0.8 respectively. After modeling, results were converted to original state.

MATLAB 7 neural network toolbox allows selecting the network type, number of hidden layers and hidden layer neurons, iterations during the model training and transfer functions. The non-linear function chosen was tan-sigmoid. The training algorithm used was Levenberg-Marquart and other functions for network were chosen as the default values of the software. Weights were initialized with random values for training. Optimal network topology was determined by developing several networks that vary only with the size of hidden layer and simultaneously observing the change in the standard error.

Results and discussion

Electrochemical degradation of MG dye has been studied in a batch reactor using catalytic oxide coated expanded mesh anode (Ti/RuO_x-TiO_x). Preliminary experiments revealed the domain of the experiment (current density, j = 0.4 – 2.2 A dm^{-2}; electrolysis time, t = 9 – 60 min; and initial dye concentration, γ_0 = 200 – 1200 mg L^{-1}) in terms of influencing factors and their range, projecting the pollutant removal phenomena.

The calibration graph drawn for dye concentration (in the wastewater) against COD was linear passing through origin. Thus, fraction reduction in concentration of MG dye wastewater was equal to the fraction removal of COD. The concentration of dye (in the wastewater) and COD were related by the equation

$$\gamma_{COD} = 2.56 \cdot \gamma_{dye} \quad (12)$$

Artificial neural network

Totally, 125 data were collected in random combination of factors in the experimental run domain for the development of ANN model. The five run data of different combinations of variables, given complete COD removal, were not considered for the ANN analysis. The remaining 120 experimental run data were divided randomly into two sets. One set, containing 108 experimental run data were used for training and the other 12 run data were used for testing the model.

Various neural networks were selected (Table 1) based on the number of weights to be determined and the available number of data for training.[21] Several iterations were conducted with different numbers of neurons of hidden layer in order to determine the best ANN structure. The trial started with the case of single hidden layer. The number of neurons in the hidden layer is varied for 3, 5, 7 and 9; the corresponding networks are notated N1, N2, N3 and N4 respectively. The least standard error value and a good prediction of the outputs of both training and validation sets were obtained with 9 neurons in the hidden layer (N4). The cases of 10 and more neurons in the hidden layer were not giving consistent results. The performance of ANN models of two hidden layer cases, 3-3-3-1, 3-3-4-1 and 3-3-5-1 (notated N5, N6 and N7 respectively) were also studied. The test results along with their performance terms such as slope, intercept, r^2 and standard error are presented in Table 2. Each network is tested for its ability in predicting the performance of the process by comparing prediction with 155 numbers of experimental observations. The results for three and four layered networks are presented in Figs. 2 and 3 respectively.

The predictability of the network is again quantified in terms of standard statistical performance evaluation measures such as standard error (SE), correlation coefficient (r), average absolute relative error (AARE), average root mean square error (RMSE), normalized mean bias error (NMBE) and scatter index (SI), expressed as:

Table 1 – *Configurations of the neural networks studied*

BPNN abbreviation	Configuration
N1	3-3-1
N2	3-5-1
N3	3-7-1
N4	3-9-1
N5	3-3-3-1
N6	3-3-4-1
N7	3-3-5-1

Table 2 – *Test of the ANN models*

S. No.	CD j/A dm^{-2}	Time t/min	IDC γ_0/mg L^{-1}	Exp.	N1	N2	N3	N4	N5	N6	N7
				COD removal, η/%							
1	0.4	60	1100	44.97	44.96	41.46	43.83	44.48	45.18	45.46	46.97
2	1.6	45	500	80.81	80.95	80.60	79.83	80.64	80.74	79.62	81.14
3	2.2	60	800	73.88	71.44	73.29	74.42	73.30	73.50	72.32	73.85
4	2.2	30	500	81.03	80.60	79.53	79.50	80.25	80.52	80.64	80.67
5	0.4	15	200	34.17	30.19	35.34	28.01	29.90	32.58	37.32	34.03
6	1.6	45	800	69.30	69.55	71.28	69.50	69.46	70.40	68.87	69.83
7	1	60	1100	54.75	54.97	52.30	53.80	52.94	54.16	53.59	54.71
8	1	45	1100	51.58	52.37	54.56	53.66	51.95	52.77	52.07	53.18
9	0.4	30	200	51.91	49.99	53.18	52.06	52.57	54.67	52.99	53.18
10	1.6	30	200	83.97	84.20	84.21	84.08	83.82	84.28	83.24	83.97
11	2.2	15	1100	44.65	49.67	46.86	45.14	45.64	44.16	45.41	45.58
12	1	60	800	63.98	62.72	61.72	64.10	62.97	63.38	64.06	63.39
slope					1.0002	0.9794	1.0409	1.0259	1.0041	0.9391	0.9769
intercept					–0.2971	1.2034	–3.0956	–2.1792	–0.1398	3.7818	1.8691
r^2					0.9830	0.9845	0.9882	0.9940	0.9954	0.9974	0.9980
standard error					2.2857	2.1338	1.9787	1.3835	1.1873	0.8383	0.7627

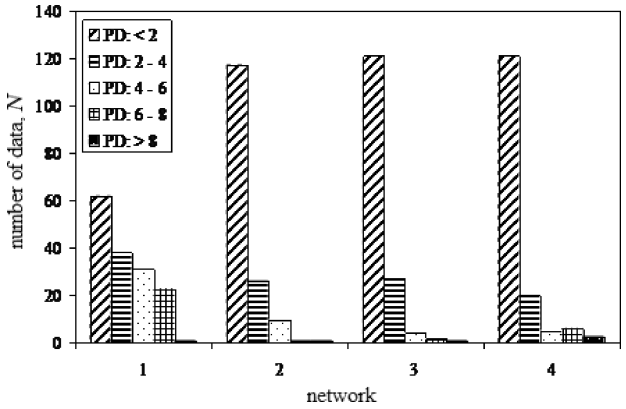

Fig. 2 – *Number of data points in five percentage deviation ranges for the case of four layered networks*

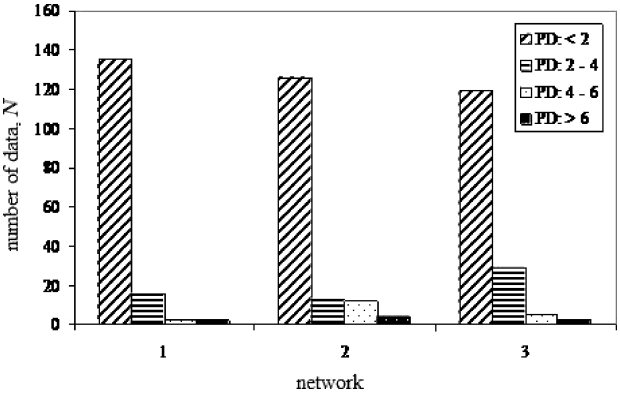

Fig. 3 – *Number of data points in four percentage deviation ranges for the case of three layered networks*

$$\mathrm{SE}=\sqrt{\frac{1}{(N-2)}\left[\Sigma(P-\overline{P})^2-\frac{[\Sigma(E-\overline{E})(P-\overline{P})]^2}{\Sigma(E-\overline{E})^2}\right]} \quad (13)$$

$$r=\frac{\sum_{i=1}^{N}(E_i-\overline{E})(P_i-\overline{P})}{\sqrt{\sum_{i=1}^{N}(E_i-\overline{E})^2\sum_{i=1}^{N}(P_i-\overline{P})^2}} \quad (14)$$

$$\mathrm{AARE}=\frac{1}{N}\sum_{i=1}^{N}\left|\frac{(E_i-P_i)}{E_i}\right|\cdot 100 \quad (15)$$

$$\mathrm{RMSE}=\left[\frac{1}{N}\sum_{i=1}^{N}(P_{ij}-E_{ij})^2\right]^{\frac{1}{2}} \quad (16)$$

$$\mathrm{NMBE}=\frac{\frac{1}{N}\sum_{i=1}^{N}(E_i-P_i)}{\frac{1}{N}\sum_{i=1}^{N}E_i}\cdot 100 \quad (17)$$

$$\mathrm{SI}=\frac{\mathrm{RMSE}}{\overline{E}} \quad (18)$$

Table 3 – *Standard statistical evaluation during validation of the model performance*

	N1	N2	N3	N4	N5	N6	N7
r	0.9951	0.9990	0.9985	0.9987	0.9993	0.9988	0.9991
AARE/%	3.1712	1.4379	1.4383	1.6627	0.9688	1.3484	1.3650
RMSE	2.2154	1.0063	1.2421	1.1428	0.7854	1.0084	0.9196
NMBE/%	–1.5869	–0.6323	0.2918	–0.4194	–0.1402	0.2808	–0.2334
SI	0.0392	0.0178	0.0220	0.0202	0.0139	0.0178	0.0163

where E is the experimental finding and P is the predicted value obtained from the neural network model. $\overline{E}$ and $\overline{P}$ are the mean values of E and P respectively. N is the total number of data employed in the investigation. The statistical terms of the networks are presented in Table 3. It can be read from Figs. 2 and 3 and their performance terms, given in Table 3, that N2, N4 and N5 are comparably better in predicting the COD removal of the process.

The correlation coefficient is a commonly used statistic and provides information on the strength of linear relationship between observed and the computed values. Higher value of *r* may not necessarily indicate better performance of ANN model[22] because of the tendency of the model to be biased towards higher or lower values. The AARE and RMSE are computed through a term-by-term comparison of the relative error and therefore are unbiased statistics for measuring the predictability of a model.[23] The NMBE gives information on the mean bias in prediction from a model. Positive NMBE indicates over prediction whereas negative indicates under prediction from a model. In the case of three layered networks, increase in number of neurons in the hidden layer enhanced the performance of the network.

It can be concluded that a single hidden layer network is adequate enough to predict the performance of the process. This observation reaffirms the universal approximation theorem that a single layer of non-linear hidden units is sufficient to approximate any continuous function. Hornik *et al.*[24] have also shown that a three-layer ANN with sigmoid transfer function can map any function of practical interest. The effects of variables on electro-oxidation of MG as predicted by ANN model N5 (3-3-3-1) are depicted in Figs. 4 and 5. It can be ascertained from the figures that the mass fraction removal of COD increases with time and current density. This can be explained that the generation of hypochlorite ion increases with current density, which eventually increases the dye degradation. The maximum COD removal can be achieved when current density and time are maximum for the given initial dye concentration. It can be observed from Fig. 6 that the fraction percentage removal of COD decreases with increase in initial dye concentration. This can be explained as, the ratio of hypochlorite ion to dye decreases with the increase in the initial dye concentration, resulting in a decreased performance.

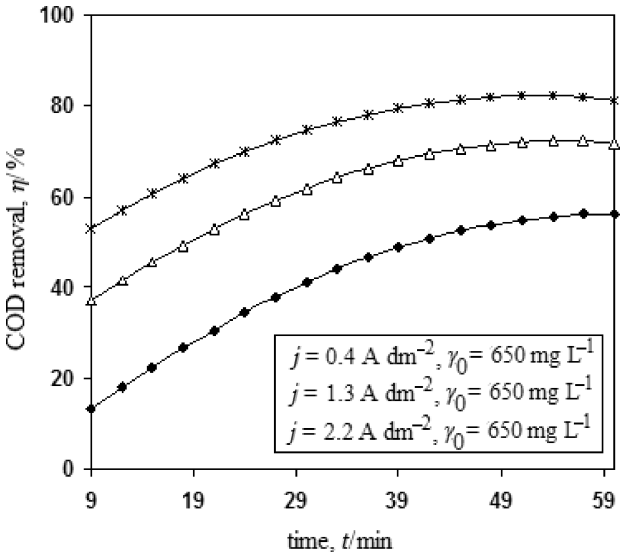

Fig. 4 – *Variation of completion on COD removal, η/% with respect to electrolysis time for different current density as predicted by N5 keeping IDC constant*

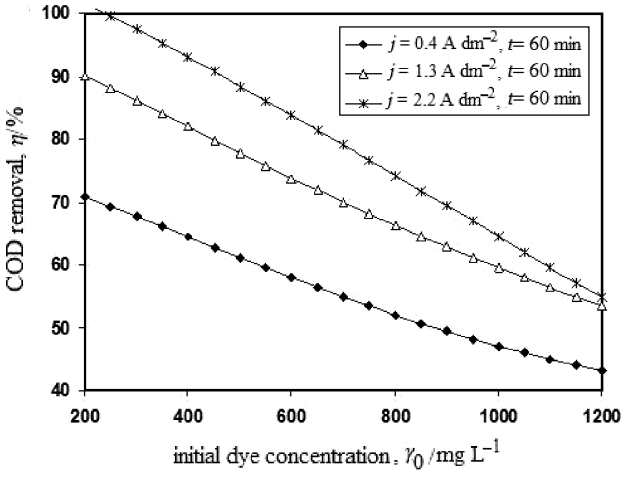

Fig. 5 – *Variation of COD removal, η/% with respect to initial dye concentration for different current density as predicted by N5 keeping electrolysis time constant*

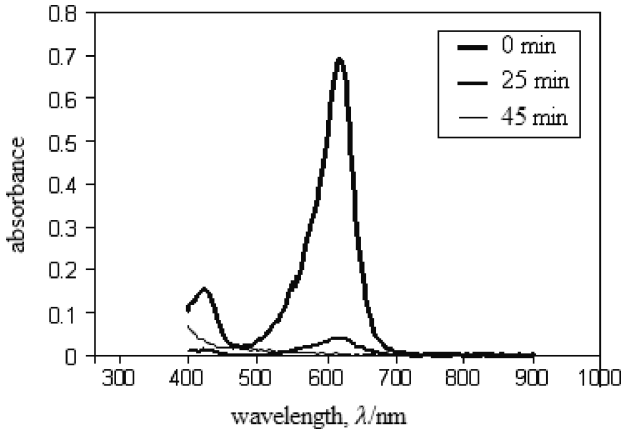

Fig. 6 – *UV/VIS spectrum of malachite green solution at various electrolysis duration (10 times diluted samples for the case of treatment at current density: 2.2 A dm^{-2} initial dye concentration: 200 mg L^{-1})*

Fig. 6 shows a typical time dependent UV/VIS spectrum of MG solution (10 times diluted samples for the case of treatment at current density, j = 2.2 A dm^{-2} and initial concentration, γ_0 = 200 mg L^{-1}). The absorbance peaks, corresponding to the dye diminished which indicated that the dye had been removed. The spectrum of MG in the visible region exhibits a main peak with a maximum at λ = 617 nm. The decrease of the absorbance peak of MG in this figure indicated a rapid degradation of the dye. The figure shows no dye remains in the wastewater of γ = 200 mg L^{-1} initial concentration after 45 minutes of treatment at a current density of j = 2.2 A dm^{-2}.

Optimization

The individual and combinations of parameters for effective degradation of MG is presented in Tables 4 and 5.

The range of individual parameters for complete removal of dye, when the other two parameters are at extreme optimal conditions in the experimental domain is given in Table 4. Therefore, current density, j = 2.01 A dm^{-2}, electrolysis time, t = 40.53 min and initial dye concentration, γ_0 = 232.04 mg L^{-1} are the best values of individual parameters when the other two parameters are at extreme optimal conditions in the experimental domain. Table 5 has been developed for combinations of two parameters giving complete removal when the third is at extreme optimal condition in the experimental domain. The r^2 values of the equations in Table 5 show that they are accurate.

Table 4 – *Optimized values of parameters for complete COD removal*

COD removal efficiency η/%	Factors		
	X_1/A dm^{-2}	X_2/min	X_3/mg L^{-1}
100	2.01 – 2.2	60	200
100	2.2	40.53 – 60	200
100	2.2	60	200 – 232.04

Conclusions

Experiments on electro-oxidation of malachite green dye effluent have been carried out in a batch electrochemical reactor, using Ti/RuO_x-TiO_x coated expanded mesh anode and stainless steel cathode. The effect of operating variables like current density, electrolysis time and initial dye concentration on COD removal was studied. The study covers conditions corresponding to COD removal from 3.75 % to 100 %. The least value of COD removal was reported at the lowest values of current density (0.4 A dm^{-2}) and electrolysis time (9 min); and highest value of initial dye concentration (1200 mg L^{-1}) in the experimental domain. Maximum dye removal is achieved when current density and electrolysis time are maximum and initial dye concentration minimum. There are many combinations of parame-

Table 5 – *Combinations of parameters for complete COD removal*

COD removal efficiency η/%	Fixed parameter			Equation	r^2 value
	X_1 j/A dm^{-2}	X_2 t/min	X_3 γ_0/mg L^{-1}		
100			200	$X_2 = 75.135 \cdot X_1^2 - 355.11 \cdot X_1 + 458.19$	0.9997
100		60		$X_3 = -134.04 \cdot X_1^2 + 733.35 \cdot X_1 - 732.58$	1
100	2.2			$X_3 = -0.3415 \cdot X_2^2 + 35.791 \cdot X_2 - 689.55$	1
100			200	$X_1 = 0.0013 \cdot X_2^2 - 0.1363 \cdot X_2 + 5.6635$	1
100		60		$X_1 = 3E\text{-}05 \cdot X_3^2 - 0.006 \cdot X_3 + 2.114$	1
100	2.2			$X_2 = 0.0013 \cdot X_3^2 - 0.3964 \cdot X_3 + 68.825$	0.9999

ters giving complete removal of dye. The individual and combinations of value of parameters giving complete degradation of the dye are reported. Current density, j = 2.01 A dm^{-2}, electrolysis time, t = 40.53 min and initial dye concentration, γ_0 = 232.04 mg L^{-1} are the best values of individual parameters for complete removal of the dye, when the other two parameters are at extreme optimal conditions in the experimental domain.

The results of this study indicate that electro-oxidation could be a feasible and effective alternative technique for the treatment of malachite green dye present in the dye house effluent of the textile industry. The single hidden layer feed-forward back-propagation neural network is found adequate enough to predict the performance of the process. The models developed can be used for scale-up.

List of symbols

A – surface area, cm^2

A_i – normalized value of X_i

E – value of experimental finding

j – current density, A dm^{-2}

N – number of data

P – predicted value from neural network

r – range limit

r^2 – correlation coefficient

t – time, min

X_i – value in uncoded terms

Greek

γ – mass concentration, mg L^{-1}

η – removal efficiency, %

λ – wavelength, nm

References

1. *Kumar, K. V., Sivanesan, S., Ramamurthi, V.,* Process Biochem. **40** (2005) 2865.
2. *Hajee, C. A. J.,* "Residues of mebendazole and malachite green in eel and trout: analytical and pharmacokinetical aspects." Doctoral Dissertation at Utrecht University Utrecht (1997) p. 183.
3. *Juttner, K., Galla, U., Schmieder, H.,* Electrochim. Acta **45** (2000) 2575.
4. *Martínez-Huitle, C. A., Brillas, E.,* Applied Catalysis B: Environmental **87** (2009) 105.
5. *Brillas, E., Sirés, I., Oturan. M. A.,* Chemical Reviews **109** (12) (2009) 6570.
6. *Korbahti, B. K.,* J. Hazard. Mater. **145** (2007) 277.
7. *Muthukumar, M., Thalamadai Karuppiah, M., Bhaskar Raju, G.,* Sep. Purif. Technol. **55** (2007) 198.
8. *Oturan, M. A., Guivarch, E., Oturan, N., Sirés, I.,* Applied Catalysis B: Environmental, **82** (2008) 244.
9. *Korbahti, B. K., Abdurrahman, T.,* J. Hazard. Mater. **151** (2008) 422.
10. *Rao, S., Mandal, S.,* Ocean Eng. **32** (2005) 667.
11. *Ahmed Basha, C., Soloman, P. A., Velan, M., Lima Rose, M., Balasubramanian, N., Siva, R.,* J. Hazardous Materials **176** (2010) 154.
12. *Awad, H. S., Galwa, N. A.,* Chemosphere **61** (2005) 1327.
13. *Comninellis, C.,* Studies in Environmental Science (Environmental Oriented Electrochemistry) **59** (1994) 77.
14. *Comninellis, C.,* Electrochimica Acta **39** (1994) 1857.
15. *Rajeshwar, K., Ibanez, J. G.,* Environmental Electrochemistry. Academic Press Inc. 1997.
16. *Raghu, S., Ahmed Basha, C.,* J. Hazard. Mater. **139** (2007) 381.
17. *Mohan, N., Balasubramanian, N., Ahmed Basha, C.,* J. Hazard. Mater. **147** (2007) 644.
18. *Subbiah, P., Krishnamurthy, S., Asokan, K., Subramanian, K., Arumugam, V.,* Indian Patent 178184, (1990).
19. *Hussain, M. A., Shafiur Rahman, M., Ng, C. W.,* J. Food Eng. **51** (2002) 239.
20. *Aber, S., Daneshvar, N., Soroureddin, S. M., Chabok, A., Asadpour-Zeynali, K.,* Desalination **211** (2007) 87.
21. *Sha, W.,* Appl. Catal. A **324** (2007) 87.
22. *Phaniraj, M. P., Lahiri, A.,* J. Mater. Process. Technol. **141** (2003) 219.
23. *Srinivasulu, S., Jain, A.,* Appl. Soft Comput. **6** (2006) 295.
24. *Hornik, K., Stinchcombe, M., White, H.,* Neural Networks **2** (5) (1989) 359.